

Assessing the impact of uniform rotation on the structure of neutron stars

Marc Salinas and J. Piekarewicz¹

¹*Department of Physics, Florida State University, Tallahassee, FL 32306, USA*

(Dated: November 7, 2024)

Driven by recent laboratory experiments and astronomical observations, significant advances have deepened our understanding of neutron-star physics. NICER’s Pulse Profile Modeling has refined our knowledge of neutron star masses and radii, while gravitational-wave detections have revealed key insights into the structure of neutron stars. Particularly relevant is the extraction of the tidal deformability by the LIGO-Virgo collaboration and the most recent determination of stellar radii by NICER, both suggesting a relatively soft equation of state (EOS) at intermediate densities. Additionally, measurements from the PREX collaboration and from pulsar timing suggest instead that the EOS is stiff in the vicinity of saturation density and at the highest densities accessible to date. But how stiff can the EOS be at these very high densities? Recent events featuring compact objects near the “lower mass gap” have raised questions about the existence of very massive neutron stars. Motivated by this finding and in light of new refinements to theoretical models, we explore the possibility that these massive objects may indeed be rapidly rotating neutron stars. We explore how rotation affects both the maximum neutron star mass and their associated radii, and discuss the implications they may have on the equation of state.

I. INTRODUCTION

In the past decade, remarkable progress has been made in our understanding of the underlying dynamics of neutron stars. In terrestrial laboratories, the recent extraction of the neutron skin thickness of ²⁰⁸Pb by the PREX collaboration [1] indicates that equation of state (EOS) in the vicinity of saturation density is stiff [2]. In the cosmos, pulsar timing observations over long time periods have determined with high precision the individual masses of a binary system consisting of a white-dwarf star and the millisecond pulsar J0740+6620 [3, 4]. With a mass of $M = 2.08 \pm 0.07 M_{\odot}$, J0740 is one of the most massive neutron stars ever measured indicating that the equation of state must be stiff at the highest densities probed in the stellar interior.

In turn, the Neutron Star Interior Composition Explorer (NICER) uses Pulse Profile Modeling to analyze X-ray emission from stellar hot spots, enabling the simultaneous determination of masses and radii. To date, four sources have been targeted: PSR J0030+0451 [5, 6], the previously mentioned millisecond pulsar PSR J0740+6620 [7, 8], the brightest rotation-powered pulsar PSR J0437-4715 [9], and PSR J1231-1411 [10]. These pioneering observations—and future ones with enhanced sensitivity—are of critical importance given that it is possible to determine the nuclear EOS from the measurement of both masses and radii [11].

Finally, the historical detection of gravitational waves emitted from the binary coalescence of neutron stars (GW170817) has opened a brand new window into our Universe [12]. Concerning the EOS, the gravitational wave signal encodes fundamental structural properties of the neutron star. The most precisely determined observable is the chirp mass, which involves a particular linear combination of the individual masses of the binary sys-

tem. Of enormous relevance but significantly harder to extract, is the combined tidal deformability ($\tilde{\Lambda}$) a quantity that also involves a linear combination of the masses but now weighted by the individual tidal deformabilities of the two stars [12]. The tidal deformability encodes the linear response of the star to the tidal field generated by the companion and is an observable highly sensitive to the stellar compactness. In particular, the relatively small tidal deformability inferred from GW170817 suggests that both stars are compact and consequently that the EOS in the relevant density regime is soft [12, 13].

Given the significant progress achieved over the last few years, one may be on the verge of determining the maximum neutron star mass. Elucidating the maximum mass is a fundamental question that has implications in astrophysics, particle physics, and nuclear physics. From the perspective of particle physics, the maximum mass configuration determines the maximum density that can exist in the stellar interior, opening the possibility for the emergence of exotic states of matter, such as color superconductors [14–16]. In the context of nuclear science, knowledge of the maximum neutron star mass constrains the nuclear dynamics at the extremes of density and isospin asymmetry, conditions that are impossible to reproduce in terrestrial laboratories. Finally, in astrophysics the answer to this question sets the scale for the minimum black-hole mass, which illuminates, among other things, the origin of the intriguing “lower mass gap” related to the absence of compact objects between three and five solar masses. Knowledge of the maximum neutron star mass also impacts the time-scale for the transition to a black hole during a binary neutron star coalescence which, in turn, affects the abundance of r-process elements.

During the last five years, the Ligo-Virgo-Kagra (LVK) collaboration has detected gravitational waves from the coalescence of compact binaries with one of the compo-

nents in, or near, the lower mass gap. The gravitational-wave event GW190814 involved the coalescence of a binary system with one of the most extreme mass ratios ever observed: a $23 M_{\odot}$ black hole and a $2.59^{+0.08}_{-0.09} M_{\odot}$ “compact” object tantalizingly near the lower mass gap [17]. More recently, the LIGO-Virgo-Kagra (LVK) collaboration reported the coalescence of a compact binary—GW230529—with the primary component having a mass of $3.6^{+0.8}_{-1.2} M_{\odot}$ [18]. In both cases, it has been suggested that the compact objects in (or near) the mass gap may be too heavy to be a neutron star [17, 18]. Nevertheless, both papers left open the possibility that the compact object in the mass gap may be a neutron star, given that gravitational-data alone cannot exclude such possibility. We note that a recent electromagnetic observation of the pulsar binary PSR J0514-4002E places the (companion) mass of the compact object at a value of 2.09 and $2.71 M_{\odot}$ [19], an interval that overlaps with the secondary object in GW190814.

Motivated by the discovery of GW190814—and given that the gravitational-wave signal by itself cannot exclude the existence of very massive neutron stars—an earlier publication explored [20] the implications of a $2.6 M_{\odot}$ neutron star on a variety of observables sensitive to the stiffness of the equation of state. It was concluded at that time that for the set of covariant energy density functionals (EDFs) explored in such a work, the stiffening of the EOS required to support super-massive neutron stars was found to be inconsistent with constraints obtained from both energetic heavy-ion collisions [21] and from the low tidal deformability inferred from GW170817 [12, 13]. So if that was the case, what has changed since then that still motivates us to explore the possibility that the primary object in GW230529—an object even more massive than the secondary object in GW190814—may be a very massive neutron star?

We provide a three-prong response to the above question. First, a recent Bayesian analysis [22] of flow data from the STAR collaboration seems to favor a hard equation of state at densities of about 2-3 nuclear matter saturation density. This is in stark contrast to the Danielewicz, Lacey, and Lynch analysis [21] that ruled out strongly repulsive equations of state. Hence, the safest conclusion to draw from these competing studies is that at present there is no robust constraint from relativistic heavy-ion collisions on the high-density component of the nuclear EOS. Thus, on the basis of heavy-ion collisions alone, there is no longer any reason to reject the stiff equation of state proposed in our analysis of GW190814 [20]. Second, although the tidal deformability extracted from GW170817 suggests a soft EOS in the vicinity of twice saturation density [13], a re-analysis of the tidal parameters by Gamba and collaborators identified systematic errors in the waveform approximants as a major issue in the inference of the tidal parameters [23]. Note that the low tidal deformability suggested in the discovery paper [13] was also used in Ref. [20] as an argument against the existence of very massive stars.

Finally and importantly, in post-Newtonian theory there is a well known degeneracy between the mass ratio and the effective spin of the binary system. This implies that the extraction of the spin of the individual components will remain a significant challenge for some time to come. And whereas GW170817 suggests a low value for the effective spin parameter based on the notion that old neutron stars had ample time to spin down, this may not always be the case. Thus, if instead one assumes that the previously identified neutron stars may be spinning very fast, then it is not the mass of the non-rotating configuration that is relevant, but rather that of the rotating configuration. As such, we will assume throughout that the inferred masses of both the secondary object in GW190814 and the primary object in GW230529 may correspond to rapidly spinning neutron stars. Moreover, we note that NICER accounts for the rotation of the millisecond pulsars by reporting the “equatorial radius”, a quantity that is often compared against theoretical predictions for static, non-rotating neutron stars. Examining the impact of rotation on both the maximum mass configuration and stellar radii is the main goal of this work.

The manuscript has been organized as follows. In Sec.II we provide a brief review of the formalism used to compute the equation of state. Model uncertainties are quantified by adopting a few parameterizations that generate both soft and stiff equations of state. In turn, these models serve as input into a TOV equation and into two publicly available codes, RNS [24, 25] and LORENE, that will serve to assess the impact of uniform rotation. Our results are presented in Sec.III and we conclude by summarizing our results in Sec.IV.

II. FORMALISM

As in much of our earlier work, covariant density functional theory will be the theoretical framework that will be employed to test the impact of rotation on the possible existence of massive neutron stars. In such a framework, a relativistic Lagrangian density consisting of nucleons and mesons is calibrated to the properties of finite nuclei and neutron stars. It is important to note that the equation of state EOS that serves as the sole input for the Tolman–Oppenheimer–Volkoff (TOV) equations is constructed from the same underlying Lagrangian density that is used to compute the properties of finite nuclei, thereby connecting nuclear phenomena with length scales that differ by more than 18 orders of magnitude.

The underlying Lagrangian density has been extensively reviewed in earlier publications [26–29], so we limit ourselves to highlight the following two terms that are of particular importance to the high-density component of the equation of state:

$$\mathcal{L}_2 = \frac{\zeta}{4!} g_{\nu}^4 (V_{\mu} V^{\mu})^2 + \Lambda_{\nu} \left(g_{\rho}^2 \mathbf{b}_{\mu} \cdot \mathbf{b}^{\mu} \right) \left(g_{\nu}^2 V_{\nu} V^{\nu} \right), \quad (1)$$

where g_v and g_ρ represent the strength of the Yukawa coupling of the nucleon to the isoscalar-vector (V^μ) and isovector-vector (\mathbf{b}_μ) meson fields, respectively. Besides the standard Yukawa couplings, the Lagrangian density includes several meson self-interacting terms to account for density dependent effects. The first term in the above expression involves a quartic term in V^μ that was introduced by Müller and Serot to modify the high density component of the EOS [30]. In particular, Müller and Serot showed that by tuning ζ , one can change the maximum mass of a neutron star by up to one solar mass—with only minimum impact on the ground state properties of finite nuclei. In turn, the second term in the Lagrangian density induces mixing in the vector channel between the isoscalar and the isovector meson fields. The main motivation behind introducing Λ_v was to soften the symmetry energy—a quantity that plays a critical role in the determination of both the neutron skin thickness of neutron-rich nuclei and the radius of neutron stars [26]. By properly tuning ζ and Λ_v , one can stiffen the EOS of symmetric matter to generate massive neutron stars while softening the symmetry energy to obtain small stellar radii and tidal deformabilities. Indeed, it was precisely this approach that gave rise to the calibration of the “BigApple” energy density functional, in the hope that one could account for the mass of the secondary object in GW190814 [20].

We close this section by listing in Table I values for ζ and Λ_v for BigApple alongside two other energy density functionals: FSUGarnet [31] and FSUGold2 [28]. The table displays predictions from these three models for stellar observables that are most sensitive to ζ and Λ_v . For example, tuning ζ to small (non-negative) values stiffens the high density component of the EOS, resulting in large maximum masses (M_{TOV}) as in the case of BigApple. In turn, increasing Λ_v softens the symmetry energy at the intermediate densities that control tidal deformabilities and stellar radii [32]. Such behavior is imprinted in the predictions of BigApple which generates both a large (M_{TOV}) and moderate stellar radii. In contrast, both FSUGarnet and FSUGold were calibrated to account for the $M_{\text{TOV}} \gtrsim 2 M_\odot$ limit, but with vastly different predictions for the stellar radius and tidal deformability of a $1.4 M_\odot$ neutron star.

Model	ζ	Λ_v	M_{TOV}	$R_{1.4}$	$\Lambda_{1.4}$
BigApple	0.00070	0.047471	2.600	12.960	717.3
FSUGarnet	0.02350	0.043377	2.066	12.869	624.8
FSUGold2	0.02560	0.000823	2.073	14.122	827.3

TABLE I. The two model parameters ζ and Λ_v , alongside model predictions for the maximum mass of the static configuration (in solar masses), the radius (in km), and tidal deformability of a 1.4 solar mass neutron star.

The results provided in Table I were obtained by solving the Tolman-Oppenheimer-Volkoff equations for a

static, non-rotating configuration. Uniform rotation—especially for rapid rotation near the mass shedding limit—requires the numerical solution of Einstein’s equations. In the next chapter, two publicly available codes will be used to assess the impact of uniform rotation on the structure of neutron stars. The Rapidly Rotating Neutron Star (RNS) code is an efficient and easy to implement code designed to study rapidly rotating, relativistic, compact stars [24, 25]. In turn, LORENE is a software package developed to solve problems in numerical relativity using spectral methods [33, 34]. Both RNS and LORENE are flexible enough to allow for the input of generic equations of state, such as the ones generated by the three covariant EDFs listed in Table I. To ensure consistency, all results that will be presented in the following section were generated using both RNS and LORENE.

III. RESULTS

A. Impact of Uniform Rotation on Stellar Radii

We start this section by assessing the impact of uniform rotation on four millisecond pulsars targeted by the NICER collaboration: PSR J0030+0451, PSR J0740+6620, PSR J0437-4715, and PSR J1231-1411, with rotational frequencies of 205 Hz [6], 346 Hz [3], 174 Hz [35], and 271 Hz [10], respectively. In Fig. 1 we display 68% and 95% credible Mass-Radius intervals for the four sources; for further details on the analysis see Ref. [36] and references contained therein. Chronologically, PSR J0030+0451 was the first targeted source. However, relative to the initial publication [5, 6], a recent reanalysis by Vinciguerra and collaborators [37] using combined NICER and XMM-Newton data found a bimodal structure that is reflected in the two contours displayed in the figure. As such, J0030 does not impose any significant constraint on the equation of state.

The next targeted source was PSR J0740+6620. Unlike PSR J0030+0451 where no mass measurement is currently available, an accurate determination of the mass of PSR J0740+6620 already existed [3, 4]. This allowed for a determination of the stellar radius without any significant change in the mass from the prior pulsar timing observation. Note that the contours for PSR J0740+6620 are from Ref. [7], as Miller et al. reported a radius with a significantly larger central value [8], although in both cases the uncertainties are large. Recently, NICER reported the mass and radius of PSR J0437-4715, the closest and brightest of the four observed sources. Benefiting from available tight priors, Choudhury and collaborators inferred a mass largely unchanged from the prior value of $M = 1.418 \pm 0.044 M_\odot$ [38], but with a relatively small radius centered at 11.36 km [9]. Finally, we include in the figure the latest observation from the NICER mission—PSR J1231-1411, a millisecond pulsar with a mass in the neighborhood of one solar mass and an equatorial radius of about 12.6 km [10]. The tight limit on the radius was

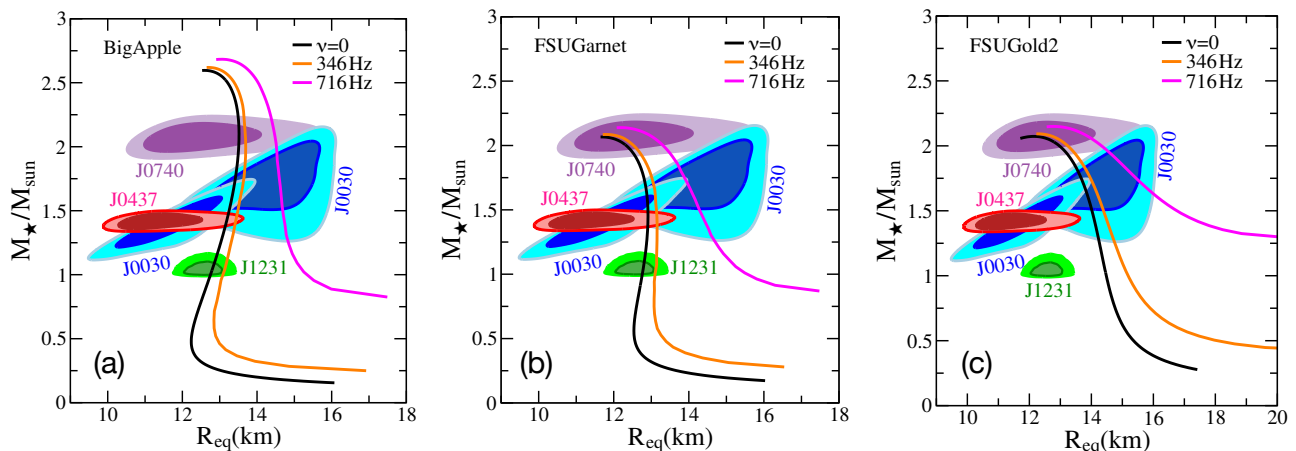


FIG. 1. NICER 68% and 95% credible mass-radius intervals for their four target sources. Also shown are predictions from the three covariant energy density functionals introduced in the text; see Table I. Predictions from these three models are made for the non-rotating configuration as well as for uniform rotation at the two frequencies listed on the inset.

obtained by demanding consistency with previous observational constraints and informed by chiral effective field theory. Instead, if the analysis used a largely uninformative prior, the equatorial radius increases by about one kilometer [10].

To confront the NICER data, we have used the three models already introduced in Table I to compute mass-radius (MR) relations. Given that NICER reports equatorial radii for all four millisecond pulsars, we provide predictions for a non-rotating configuration ($\nu = 0$) together with predictions for uniform rotation at 346 and 716 Hz. We selected 346 Hz for being the highest frequency of the four NICER sources, while 716 Hz as the frequency of PSR J1748-2446ad, the fastest known spinning pulsar observed to date [39]. In Figure 1(a) we display predictions from BigApple, a covariant energy density functional constructed with the sole purpose of exploring the possibility of generating very massive neutron stars [20]. As seen in the figure, the model without rotation already predicts a maximum mass for the static configuration of $M_{\text{TOV}} = 2.6 M_{\odot}$; see also Table I. As far as stellar radii, the model is consistent with all four NICER sources, although falls within the 95% contour for PSR J0437. Uniform rotation at $\nu = 346$ Hz has a negligible effects for the highest mass and only marginal impact at intermediate masses. Instead, neutron stars spinning at the highest frequency of $\nu = 716$ Hz, continue to have a minimal impact on the maximum mass but an appreciable effect on stellar radii, especially for low-mass stars. This is highly relevant given the relatively low mass of PSR J1231-1411 [10]. Although PSR J1231-1411 rotates at “only” 271 Hz, we observe in Fig.1(a) that the equatorial radius of a putative low mass pulsar rotating at 716 Hz could increase by more than 2 km.

The impact of uniform rotation on the other two models—FSUGarnet and FSUGold2—is qualitatively similar. Note that these two models were calibrated by demanding that they both satisfy the 2-solar mass con-

straint, but not more. The main difference between these two models is their prediction for the density dependence of the symmetry energy; FSUGarnet is soft whereas FSUGold2 is stiff. As such, FSUGold2 predicts both thick neutron skins and large stellar radii. Although consistent with J0030 and J0740, both J0437 and J1231 already rule out the large stellar radii predicted by FSUGold2. Note that for a model as stiff as FSUGold2, the shedding mass frequency is less than 716 Hz for neutron stars with masses below $1.3 M_{\odot}$. Interestingly, with a prediction of $R_{\text{skin}}^{208} = 0.287 \pm 0.020$ fm for the neutron skin thickness of ^{208}Pb [28], FSUGold2 is entirely consistent with the experimental value of $R_{\text{skin}}^{208} = 0.283 \pm 0.071$ fm published by the PREX collaboration [1]. This could suggest a significant softening of the equation of state between one and three times nuclear saturation density [2].

B. Impact of Rotation on Maximum Masses

Whereas in the previous section we examined the impact of a “modest” rotation on the mass-radius relation, in this section we explore its impact on stellar masses at the mass shedding limit.

We start with a simple exercise that assumes that realistic models, such as the ones that we have introduced, can be pushed to such an extreme to generate maximum masses up to $M_{\text{TOV}} = 2.8 M_{\odot}$, as demonstrated in Ref. [30]. To assess the impact of maximum uniform rotation on the stability of the star, we evolve the static configuration by adopting a constant value for the ratio of masses, as suggested in the recent analysis of Musolino, Ecker, and Rezzolla [40]; that is,

$$\mathcal{R} \equiv \frac{M_{\text{max}}}{M_{\text{TOV}}} = 1.255_{-0.040}^{+0.047}, \quad (2)$$

where M_{TOV} is the maximum mass of the non-rotating

(static) configuration and M_{\max} is the maximum mass of the stable, uniformly rotating configuration.

The probability distribution function (PDF) of the maximum mass configuration M_{\max} may now be obtained from a “product normal distribution” defined as [?]:

$$P(M_{\max}) = \int_{-\infty}^{\infty} P(\mathcal{R})P(M_{\text{TOV}}) \frac{dM_{\text{TOV}}}{|M_{\text{TOV}}|}, \quad (3)$$

where in the above expression \mathcal{R} is the ratio of the two masses given in Eq.(2). Alternatively, one can generate the product normal distribution for $M_{\max} = \mathcal{R} \cdot M_{\text{TOV}}$ by simply using Monte Carlo methods to sample from both $P(\mathcal{R})$ and $P(M_{\text{TOV}})$ distributions.

However, a drastic simplification follows in the limit that the width of at least one of the two probability distributions is vanishingly small. For example, in the limit that the theoretical uncertainties in M_{TOV} can be ignored [28], the product normal distribution reduces to a normal distribution with the following mean and standard deviations: $\mu_{\max} = \mu_{\mathcal{R}} \cdot \mu_{\text{TOV}}$ and $\sigma_{\max} = \sigma_{\mathcal{R}} \cdot \mu_{\text{TOV}}$. Mean values and standard deviations computed in this manner are listed in Table II.

M_{TOV}	M_{\max}	$\langle \Delta M_{\max} \rangle$	P_{NS}
2.20	2.761(088)	-0.811	0.12
2.40	3.012(096)	-0.562	0.19
2.60	3.263(104)	-0.306	0.28
2.80	3.514(112)	-0.057	0.42

TABLE II. Assumed maximum mass of the static configuration M_{TOV} and the resulting mean value and standard deviation for the mass of the maximally stable rotating configuration. The third column displays the average value of the $M_{\max} - M_{\text{LVK}}$ distribution. The last column displays the probability that the primary object in GW230529 be a neutron star. All masses are in solar masses.

Probability distribution functions are shown in Fig. 2(a) for GW190814 [17], for GW230529 [18], and for the maximum mass of the uniformly rotating configuration assuming a model that can support a static configuration with a maximum mass of $M_{\text{TOV}} = 2.6 M_{\odot}$, as in the case of BigApple. Note that the PDF for GW190814 has been divided by a factor of 2.

Having generated the theoretical distribution of maximum masses, we can now generate a distribution for the mass difference between M_{\max} and M_{LVK} , where M_{LVK} is either the secondary object in GW190814 or the primary object in GW230529. In this manner one frames the question of whether the enigmatic compact object is a neutron star as follows: what is the probability that the difference $\Delta M_{\max} \equiv M_{\max} - M_{\text{LVK}}$ be positive? In the case of the secondary object in GW190814, the answer is evident from Fig. 2(a), namely, the probability that the compact object is a neutron star is one. In the case of the primary object in GW230529, the answer is not evident because both the central value and the uncertainty

are large. Hence, we display in Fig. 2(b) the probability distribution $P(\Delta M_{\max})$. The area under the curve to the right of the origin represents the probability that the primary object in GW230529 be a neutron star; to the left that it is a black hole. Hence, under the assumed conditions, there is a 28% probability that the primary object in GW230529 is a neutron star. Averages values for $P(\Delta M_{\max})$ and the probability that the primary object in GW230529 for various assumed values for M_{TOV} are listed in Table II.

Although the schematic results displayed in Table II and Fig. 2 provide credible estimates for the probability that the primary object in GW230529 be a neutron star, we now examine the effects of rotation on the three covariant EDFs considered in this work. We list on the second and third columns of Table III the maximum mass (in solar masses) and its associated radius (in km) for the non-rotating configuration. In turn, the last three columns display the Kepler frequency (in kHz) together with the mass and radius of the resulting maximally stable rotating configuration, with the increase in the corresponding quantities shown in parenthesis. Whereas the $\sim 20\%$ increase in $\mathcal{R} = M_{\max}/M_{\text{TOV}}$ is consistent with the estimate from Ref. [40], it is interesting that the increase in the equatorial radius is even larger. Clearly, any observable highly sensitive to the stellar compactness, such as the tidal deformability, will be highly affected.

Model	M_{TOV}	R_{TOV}	ν_{K}	M_{\max}	R_{\max}
BigApple	2.596	12.590	1.481	3.208(24%)	16.727(33%)
FSUGarnet	2.066	11.690	1.409	2.519(22%)	16.048(37%)
FSUGold2	2.073	12.151	1.321	2.463(19%)	16.609(37%)

TABLE III. Maximum mass (in M_{\odot}) for the non-rotating and maximally stable rotating configurations and their corresponding equatorial radii (in km), with the Kepler frequency ν_{K} given in kHz. The percentages denote the increase in mass and radius in going from the non-rotating to the rotating configuration.

We conclude this section by examining the impact of uniform rotation on the structure of neutron stars away from the mass shedding limit. This is motivated by the fact that at present there is no evidence that neutron stars could spin at—or even near—the mass shedding limit. For example, electromagnetic observations of millisecond pulsars place the limit for maximum rotation at 716 Hz [39], a value that is significantly smaller than any of the Kepler frequencies listed in Table III. Second, although difficult to determine, the spin of the individual components of coalescing neutron stars that merge over long period of times is expected to be low. Hence, we display in Fig. 3 the evolution of the maximum mass as a function of frequency. Also shown are the masses for the secondary object in GW190814 [17], the primary object in GW230529 [18], and for the companion mass of the

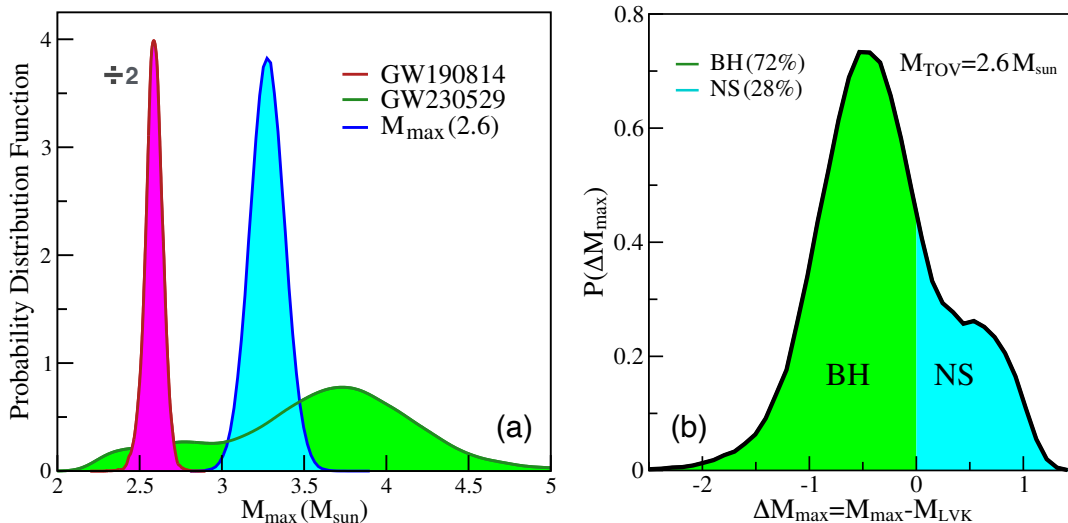


FIG. 2. (a) Probability distribution functions for the secondary object in GW190814 (divided by 2) and for the primary object in GW230529. Also shown is the impact of uniform rotation at the mass shedding limit on a star with a TOV mass of $2.6 M_{\odot}$, with the rotational enhancement adopted from Eq.(2). (b) Probability distribution function for the difference between M_{\max} and the mass of the primary object in GW230529.

millisecond pulsar PSR J0514 [19]. The figure shows a slow evolution at low frequencies that is then followed by a fairly rapid increase in the vicinity of the Kepler limit. This is consistent with the results displayed in Fig.1 that show no dramatic increase in the mass up to about half Ω_{Kepler} . However, we underscore that the impact of rotation on stellar radii could be significant. Finally, we note that the predictions from BigApple at all frequencies—even in the static limit—are consistent with the three sources displayed in the figure, suggesting that at this time it is difficult to rule out that the unidentified compact objects may be neutron stars.

IV. CONCLUSIONS

The nature of matter at extreme temperatures and densities remains one of the most fundamental questions in nuclear astrophysics. Observations of massive neutron stars and their binary mergers play a critical role in answering this question. The determination of a neutron star’s maximum mass and its associated radius provides powerful constraints on the maximum density achievable in its interior. In turn, this information serves as a cornerstone for validating the many fascinating phases that have been conjectured to exist in the stellar interior, such as quark and/or hyperonic matter.

In this work, we have examined available posterior distributions for the primary compact object in GW230529 and assessed its possibility of being a rapidly rotating neutron star. Under the framework of covariant density functional theory, models such as BigApple—that are compatible with nuclear physics observables—place the upper limit on this probability at around 28% for

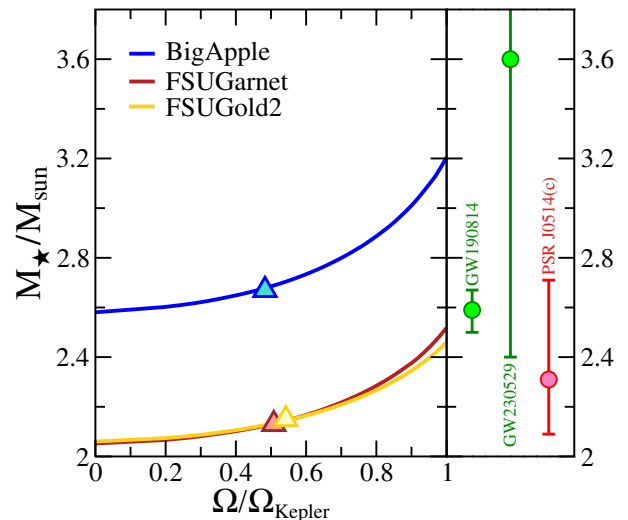


FIG. 3. Evolution of the maximum mass as a function of rotational frequency for the three covariant models considered in this paper. The triangles denote rotation at the maximum observed limit of 716 Hz. The right-hand panel displays central values and uncertainties for three heavy compact objects that fall in (or near) the lower mass gap.

the maximally rotating configuration (see Fig.2). Despite this relatively low probability, our analysis suggests that the rapid rotation of neutron stars can substantially increase their maximum mass, opening the possibility that massive neutron stars, such as the one in GW230529, could indeed exist in the lower mass gap.

Moreover, our analysis on the uniform rotation of neutron stars seem to suggest that models consistent with nuclear physics may also be able to accommodate very

heavy neutron stars—even in the absence of rotation. Indeed, as shown in Fig.3, the maximum mass predicted by BigApple for the non-rotating configuration accommodates the large mass of the secondary component of GW190814. This suggests that static configurations of neutron stars could also account for the existence of these massive compact objects, challenging previous assertions that such high masses necessarily imply black hole formation.

While our initial motivation was on how rotation affects neutron star masses, we discovered even more significant changes to stellar radii. This finding is particularly relevant to the NICER mission and future X-ray telescopes that target millisecond pulsars. For instance, our results revealed that the equatorial radius of a millisecond pulsar with a mass of approximately one solar mass rotating at the current maximum observed frequency, can vary by a few kilometers (see Fig.1).

Although significant uncertainties remain, particularly regarding the high density behavior of nuclear matter, our results affirm the potential for very massive neutron stars in the lower mass gap, both with and without rotation. These findings underscore the need for more precise constraints on the nuclear equation of state, especially

at densities beyond saturation. Future experiments at the Facility for Rare Isotope Beams will allow laboratory studies of asymmetric nuclear matter at twice normal nuclear density. Moreover, cosmic observations, such as those from next-generation gravitational wave detectors and improved Pulse Profile Modeling, will be crucial in further constraining the mass-radius relation, assessing the impact of rotation on the structure of neutron stars, and validating the existence—or lack-thereof—of a lower mass gap.

ACKNOWLEDGMENTS

We thank the ECT* and the FRIB Theory Alliance for support at the DTP/TALENT School on Nuclear Theory for Astrophysics during which this work was initiated. We would also like to thank our colleagues Devarshi Choudhury, Anna Puecher, Tuomo Salmi, and Serena Vinciguerra for many stimulating discussions, and Prof. Frederi Viens for valuable insights into the statistical analysis. This material is based upon work supported by the U.S. Department of Energy Office of Science, Office of Nuclear Physics under Award Number DE-FG02-92ER40750.

-
- [1] D. Adhikari *et al.* (PREX), *Phys. Rev. Lett.* **126**, 172502 (2021).
 - [2] B. T. Reed, F. J. Fattoyev, C. J. Horowitz, and J. Piekarewicz, *Phys. Rev. Lett.* **126**, 172503 (2021).
 - [3] H. T. Cromartie *et al.*, *Nat. Astron.* **4**, 72 (2019).
 - [4] E. Fonseca *et al.*, *Astrophys. J. Lett.* **915**, L12 (2021).
 - [5] T. E. Riley *et al.*, *Astrophys. J. Lett.* **887**, L21 (2019).
 - [6] M. C. Miller *et al.*, *Astrophys. J. Lett.* **887**, L24 (2019).
 - [7] T. E. Riley *et al.*, *Astrophys. J. Lett.* **918**, L27 (2021).
 - [8] M. C. Miller *et al.*, *Astrophys. J. Lett.* **918**, L28 (2021).
 - [9] D. Choudhury *et al.*, *Astrophys. J. Lett.* **971**, L20 (2024).
 - [10] T. Salmi *et al.*, (2024), arXiv:2409.14923 [astro-ph.HE].
 - [11] L. Lindblom, *Astrophys. J.* **398**, 569 (1992).
 - [12] B. P. Abbott *et al.* (Virgo, LIGO Scientific), *Phys. Rev. Lett.* **119**, 161101 (2017).
 - [13] B. P. Abbott *et al.* (Virgo, LIGO Scientific), *Phys. Rev. Lett.* **121**, 161101 (2018).
 - [14] M. G. Alford, K. Rajagopal, and F. Wilczek, *Phys. Lett. B* **422**, 247 (1998).
 - [15] M. G. Alford, K. Rajagopal, and F. Wilczek, *Nucl. Phys.* **B537** (1999).
 - [16] M. G. Alford, A. Schmitt, K. Rajagopal, and T. Schafer, *Rev. Mod. Phys.* **80**, 1455 (2008).
 - [17] R. Abbott *et al.* (LIGO-Virgo Collaboration), *Astrophys. J.* **896**, L44 (2020).
 - [18] A. G. Abac *et al.* (The LIGO Scientific Collaboration, the Virgo Collaboration, and the KAGRA Collaboration), *Astrophys. J.* **970**, L34 (2024).
 - [19] E. D. Barr *et al.*, *Science* **383**, 275 (2024).
 - [20] F. J. Fattoyev, C. J. Horowitz, J. Piekarewicz, and B. Reed, *Phys. Rev. C* **102**, 065805 (2020).
 - [21] P. Danielewicz, R. Lacey, and W. G. Lynch, *Science* **298**, 1592 (2002).
 - [22] D. Oliinychenko, A. Sorensen, V. Koch, and L. McLerran, *Phys. Rev. C* **108**, 034908 (2023).
 - [23] R. Gamba, M. Breschi, S. Bernuzzi, M. Agathos, and A. Nagar, *Phys. Rev. D* **103**, 124015 (2021).
 - [24] N. Stergioulas and J. L. Friedman, *Astrophys. J.* **444**, 306 (1995).
 - [25] N. Stergioulas, *Living Rev. Rel.* **6**, 3 (2003).
 - [26] C. J. Horowitz and J. Piekarewicz, *Phys. Rev. Lett.* **86**, 5647 (2001).
 - [27] B. G. Todd-Rutel and J. Piekarewicz, *Phys. Rev. Lett.* **95**, 122501 (2005).
 - [28] W.-C. Chen and J. Piekarewicz, *Phys. Rev.* **C90**, 044305 (2014).
 - [29] J. Yang and J. Piekarewicz, *Ann. Rev. Nucl. Part. Sci.* **70**, 21 (2020).
 - [30] H. Mueller and B. D. Serot, *Nucl. Phys.* **A606**, 508 (1996).
 - [31] W.-C. Chen and J. Piekarewicz, *Phys. Lett.* **B748**, 284 (2015).
 - [32] J. M. Lattimer and M. Prakash, *Phys. Rept.* **442**, 109 (2007).
 - [33] S. Bonazzola, E. Gourgoulhon, and J.-A. Marck, *Phys. Rev. D* **58**, 104020 (1998).
 - [34] E. Gourgoulhon, P. Haensel, R. Livine, E. Paluch, S. Bonazzola, and J. A. Marck, *Astron. Astrophys.* **349**, 851 (1999).
 - [35] V. Sosa Fiscella *et al.*, *Astrophys. J.* **908**, 158 (2021).
 - [36] K. Chatziioannou, H. T. Cromartie, S. Gandolfi, I. Tews, D. Radice, A. W. Steiner, and A. L. Watts, (2024), arXiv:2407.11153 [nucl-th].
 - [37] S. Vinciguerra *et al.*, *Astrophys. J.* **961**, 62 (2024).
 - [38] D. J. Reardon *et al.*, *Astrophys. J. Lett.* **971**, L18 (2024).
 - [39] J. W. T. Hessels, S. M. Ransom, I. H. Stairs, P. C. C.

Freire, V. M. Kaspi, and F. Camilo, *Science* **311**, 1901 (2006).

[40] C. Musolino, C. Ecker, and L. Rezzolla, *Astrophys. J.* **962**, 61 (2024).